Interfacial improvement of poly (lactic acid)/tannin acetate composites via radical initiated polymerization

Jingjing Liao, Nicolas Brosse, Sandrine Hoppe, Xiaojian Zhou, Xuedong Xi, Guanben Du, Antonio Pizzi

Interfacial improvement of poly (lactic acid)/tannin acetate composites via radical initiated polymerization

Jingjing LIAO [1,2,3,4], Nicolas BROSSE [3,*], Sandrine HOPPE [4], Xiaojian ZHOU [1,*], Xuedong XI [3], Guanben DU [1,2,*], Antonio PIZZI [3]

[1] *Yunnan Provincial Key Laboratory of Wood Adhesives and Glued Products, Southwest Forestry University, Kunming 650224, Yunnan, P. R. China*

[2] *College of Materials Science and Technology, Beijing Forestry University, 35 Tsinghua East Road. Haidian District, Beijing,100083, P. R. China*

[3] *LERMAB, University of Lorraine, Boulevard des Aiguillettes BP 70239,54506 Vandœuvre-lès-Nancy, France ;*

[4] *LRGP, University of Lorraine, 1, Rue Grandville, BP 451, 54001 Nancy Cedex, France;*

** Correspondences: xiaojianzhou@hotmail.com (X. Zhou) ; gongben9@hotmail.com (G. Du) ; nicolas.brosse@univ-lorraine.fr (N. Brosse).*

Abstract: A wholly bio-composite based on poly (lactic acid) (PLA) and tannin acetate was successfully prepared via in situ reactive extrusion using dicumyl peroxide (DCP) to improve interfacial adhesion. The composites based on PLA and tannin acetate with high acetylation degree exhibited increased molecular weight as compared with reactive extruded PLA, together with the improvement of Young's modulus and tensile strength. The rheology results showed that reactive extruded PLA/tannin acetate composites exhibited increased complex viscosity and modulus storage, indicating the strong interfacial adhesion of PLA and tannin acetate. Besides, Glass transition temperature, thermal stability, and crystallinity degree were all enhanced as a result of better interaction by radical initiated polymerization. From contact angle data, free radical extruded composites had a more hydrophobic characteristic compared with PLA, which might be interesting for food packaging application. This approach opens up a pathway to diversify the applications of tannin as a component for bio-composite preparation.

Keywords: poly (lactic acid); tannin acetate; peroxide; reactive extrusion; bio-composite

1. Introduction

Biodegradable polymers from renewable resources have been attracted great interests in past years driven by the depletion of non-renewable petroleum resources and accumulation of non-degradable plastics. Poly (lactic acid) (PLA) is a biodegradable polyester produced from agricultural products (e.g. corn, sugar cane, and sugar beet) with potential applications ranged from biomedical devices to traditional applications in plastics and composites (Ren, 2011). Wholly bio-composites based on PLA and biopolymers have been widely studied due to the low environmental impact and specific functions. For instance, nanocellulose is a good reinforcing component for PLA and it displays excellent oxygen and water vapour barrier properties of resulting composite products (Karkhanis et al., 2018; Yu et al., 2017). Phenolic compounds such as lignin generally exhibit functional properties like thermal stability, anti-UV capacity, and flame retardancy (Kumar et al., 2019; Song et al., 2018; Yang et al., 2020).

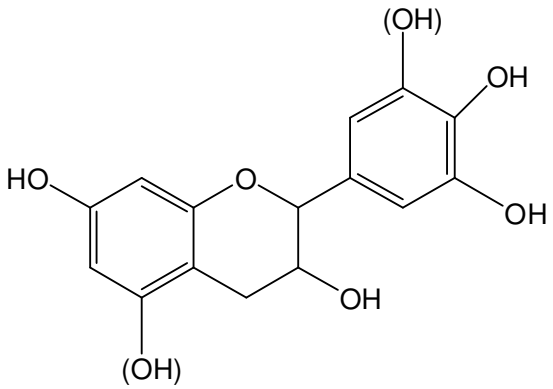

Figure 1. Simple structure of flavonoid unit of condensed tannins

Condensed tannins, composed of flavonoid units (Figure 1), are one of the most important phenolic compounds and highly abundant in bark (Pizzi, 1980). They have a range of inherent properties including UV resistance, antioxidant capacity, and antimicrobial activity, which could be considered to design PLA-based composites for outdoor, agricultural, food packaging, and medical applications. The main challenges for the preparation of PLA-tannin composites are the poor dispersion and low compatibility of tannins in PLA, which results in negative effects on mechanical properties (Anwer et al., 2015; García et al., 2016) and functional performances of the resulting composites (Liao et al., 2019a, 2019b). The widely reported strategies to overcome these disadvantages including the introduction of less hydrophilic

functional groups to tannin and synthesis tannin-based copolymer. For example, anhydride esterification of tannin was widely used for enhancing its miscibility with bioplastics (Grigsby et al., 2014, 2013; Grigsby and Kadla, 2014; Liao et al., 2020b). Tannin was also reported to copolymerize with polycaprolactone (Song et al., 2016) before blending with PLA for biomedical applications (Jiang, 2017). Unfortunately, a decrease in mechanical properties and thermal stability were observed due to noninteraction between PLA and tannin (García et al., 2016; Liao et al., 2020b). In addition, phase separation was found during 3D printing process (Liao et al., 2020b).

Inducing molecular interactions between tannin oligomers and PLA via trans-esterification were presented for achieving a strong interfacial adhesion between two phases (Bridson et al., 2018; Grigsby and Kadla, 2014). Grafting copolymerization can be also applied to induce covalent bonding in polymer blends, including ring-opening copolymerization (Song et al., 2016), ion-initiated polymerization (Luo et al., 2014, 2013) and radical initiated polymerization (Wei et al., 2015). The latter is considered as a simple and powerful approach of enhancing interfacial adhesion, since it is performed in the molten state with only minor amount of peroxide and neither special device nor extra purification step is required. This peroxide initiated reactive grafting method has been successfully applied into PLA/cellulose (Dhar et al., 2016; Zhou et al., 2018), PHB/cellulose (Wei et al., 2015) and poly(3-hydroxybutyrate-co-3-hydroxyvalerate) (PHBV)/lignin blends (Luo et al., 2016) to form covalent bonding between two phases. However, no literature regarding radical initiated polymerization of PLA/tannin has been reported yet for improving the performance of bio-composite based on PLA and tannin.

In this work, low concentrations of DCP was used as an initiator to induce grafting copolymerization between PLA and tannin for improving their interfacial adhesion. Acetylation of tannin hydroxyl groups was required to enhance dispersion and also to reduce antioxidant character of tannin, guaranteeing free radical reaction (Luo et al., 2014, 2013, 2016). The radical initiated polymerization of PLA with tannin acetate in different acetylation degree on the mechanical property, degree of crystallinity, thermal behaviour and contact angle of resulting composites were investigated.

2. Materials and methods

2.1. Materials

Poly (lactic acid) was purchased from Natureworks LLC (Minnesota, USA) and with a melt flow index of 7-9 g/10 min (210°C, 2.16 kg), which trademarked under the name IngeoTM Biopolymer (Grade 3D850). Mimosa tannins with molecular weight range from 400 Da to 1700 Da (Thébault et al., 2015) were obtained from Silva Chimica, Mondovi, Italy. Acetic anhydride (AR grade), dicumyl peroxide (DCP, 98%), acetone (AR grade) were purchased from Sigma-Aldrich (France). Pyridine was AR grade from Acros-Organics. All chemicals are used without any further purification.

2.2. Sample preparation

2.2.1. Tannin acetylation

In order to obtain tannin with less hydroxyl functional groups, mimosa tannin was initially reacted with acetic anhydride at a round bottom flask fitted with a condenser. Partially and totally acetylated tannin were achieved by using pyridine as catalyst. Continuous stirring was undertaken in the mixture with a magnetic stirrer at 60°C for 6 h (Nicollin et al., 2013). The suspension was precipitated in iced water after acetylation and centrifuged to separate the solution. The collected tannin acetate (AT) powders were washed 5 times with distilled water and air-dried for several days at room temperature. The reaction ratio, catalyst concentration, isolated yield, and degree of substitution (DS) for tannin acetylation reaction were presented in Table 1. The DS is calculated using NMR integration (Bridson et al., 2013; Luo et al., 2010; Thébault et al., 2015). The samples noted as PAT and TAT are tannin acetate with and without OH groups, respectively.

Table 1. Reaction formula of tannin acetate

Product	tannin: acetic anhydride	Pyridine (wt%)	Yield (%)	DS
PAT	1:5	1	69.3% ± 0.3	3.5
TAT	1:5	5	95.3% ± 0.2	6.3

Notes: ^{1}H-NMR spectroscopy and related NMR integration were presented in supplementary material, Figure S1.

2.2.2. Composite preparation

PLA pellet was ground into powder and blended with tannin acetate in a weight ratio of 90:10. Each formula was pre-treated with acetone-water solution (80 wt%) of dicumyl peroxide (DCP) (8 mg/ml) using 0.3 wt% based on under manually stirring at

room temperature. This concentration of DCP was chosen based on the literature (Yamoum et al., 2017) to guarantee the increased viscosity caused by free radical reaction of PLA will not affect the processability during extrusion. The pre-treated samples were left in a fume hood at room temperature for several hours until acetone evaporated, then, followed by oven-dried at 80°C for 24 hours. The PLA/PAT and PLA/TAT mixtures coated with DCP were labelled as PLPAT and PLTAT, respectively. PLA with DCP was prepared as a control sample, maned as PLD.

The melt blending of each formula was carried out in a twin-screw extruder (Thermo Scientific^{TM} Process 11, Villebon-sur-Yvette, France) with a screw rotation speed of 100 rpm and the resident time was approximately 4 min. The temperature of the extrusion was 185°C. Two mixing zones were also set in the screw profile for the purpose of effective mixing and reaction between each component. All the extruded materials were grinded into small particles for further use.

2.4. Characterizations

Proton nuclear magnetic resonance (^{1}H-NMR) spectra was recorded on a Bruker AVANCE III HD 300MHz instrument (Switzerland). DMSO was used as a solvent for tannin and acetylated tannin.

The tensile property was carried out using Instron tensile testing machine (model 5569, Norwood, MA, USA) with a 50 kN load cell and a cross-head speed of 1 mm/min at room temperature. The tensile test specimens (dumbbell-shaped, ISO 527, type 1A) were processed by a micro-compounder (Micro 15, DSM Xplore, Sittard, Netherlands) and a micro-injection molder (Xplore, Sittard, Netherlands). Four specimens were tested in each formula, and the average value and standard deviation were considered.

Molecular weight distributions of samples were measured by size-exclusion chromatography (SEC) using a Styragel column (HR-4) from Waters, with tetrahydrofuran (THF) as a solvent at a flow rate of 1.0 mL/min. The molecular weights ($\bar{M}_w$ and $\bar{M}_w$) and polydispersity index ($\bar{M}_w/\bar{M}_n$) were calculated from SEC curves using a calibration curve from standard polystyrene.

Rheological properties of extruded materials were analyzed on a rheometer (TA instrument, G2 ARES, New Castle, DE, USA) with 25 mm diameter and 1 mm gap under a nitrogen atmosphere. Dynamic strain sweep tests were performed at 1 rad/s,

in a range of 0.1-1000% to determine the linear viscoelastic region (LVR). According to the LVR, 10% strain was chosen for frequency tests. Dynamic frequency sweep tests were performed over an angular frequency range of 0.1-623.3 rad/s at 190°C.

The differential scanning calorimeter (DSC) was performed with a Metter Toledo DSC 1 (Columbus, Ohio, USA). Samples (3-4 mg) were placed in aluminium crucibles heated from -10 to 220°C at a scanning rate of 10 °C/min and kept for 2 min to ease the thermal history under a nitrogen atmosphere (50 mL/min). Then cooled to -10°C and reheated to 220°C with the same scanning rate. The crystallinity (X_c) was calculated from the values of second ramp by the following equation (1):

$$X_c(\%) = \frac{\Delta H_m - \Delta H_c}{\Delta H_m^0 \times w} \times 100\% \quad (1)$$

where ΔH_m is enthalpy of melting, ΔH_c is the enthalpy of cold crystallization, ΔH_m^0 is the enthalpy of melting for 100% crystallized PLA (93.7 J/g) (Yamoum et al., 2017), and w is the weight fraction of PLA.

Thermogravimetric analysis (TGA) was carried out with a Metter Toledo TGA/DSC (Columbus, Ohio, USA). The samples (6–7 mg) were heated from 30 to 600 °C at a heating rate of 10 °C/min under air atmosphere (50 mL/min).

Static contact angle was performed using a Ramé-Hart manual contact angle goniometer (Netcong, USA) by depositing a drop of Millipore water on the surface of specimens ($\sim 2 \times 2$ cm^2) at various locations. Each measurement was repeated at three times.

3. Results and discussion

3.1. Plausible reaction mechanism

The plausible reaction mechanism of PLA/AT composites using DCP as a free radical initiator during melt extrusion is illustrated in Scheme 1. During reactive extrusion, DCP initially decomposed into cumyloxy radicals at high temperature (around 180 °C), following by the formation of methyl radicals and acetophnone by β-scission (Scheme 1, I). These radicals tend to abstract the protons from both PLA and tannin acetate, and initiate grafting reaction between two phases to form PLA-tannin acetate copolymers by C-C cross-links. In the case of PLA, free radicals are liable to attract any theriary -CH along the PLA backbone (Scheme 1, II) (Wei and McDonald, 2015). According to the study of Wei et al., DCP radicals could attack the cellulose at different positions during extrusion, generating carbon radicals on

glucopyranose ring and alkoxy radicals on OH groups according to the ESR results (Wei and McDonald, 2015). Thus, hydrogen possibly abstracted from the residual free phenolic OH groups since the relatively weak bond dissociation energy of phenolic O-H bond (Quideau et al., 2011) and from phenyl and heterocyclic ring of flavonoid units (Scheme 1, II). With the consideration of the formation of quinonic structures from phenolic OH groups is less active (Luo et al., 2018), in situ peroxide radicals initiated covalent linkages of PLA/AT composites are possible between phenyl/heterocyclic ring of flavonoid units and PLA backbones. The possible covalent bonding between PLA-PAT and PLA-TAT was shown in Scheme 1, III.

Scheme 1. Mechanism of DCP decomposition (I); hydrogen abstraction from PLA and tannin acetate (II); potential grafting mechanism of PLA and tannin acetate (III)

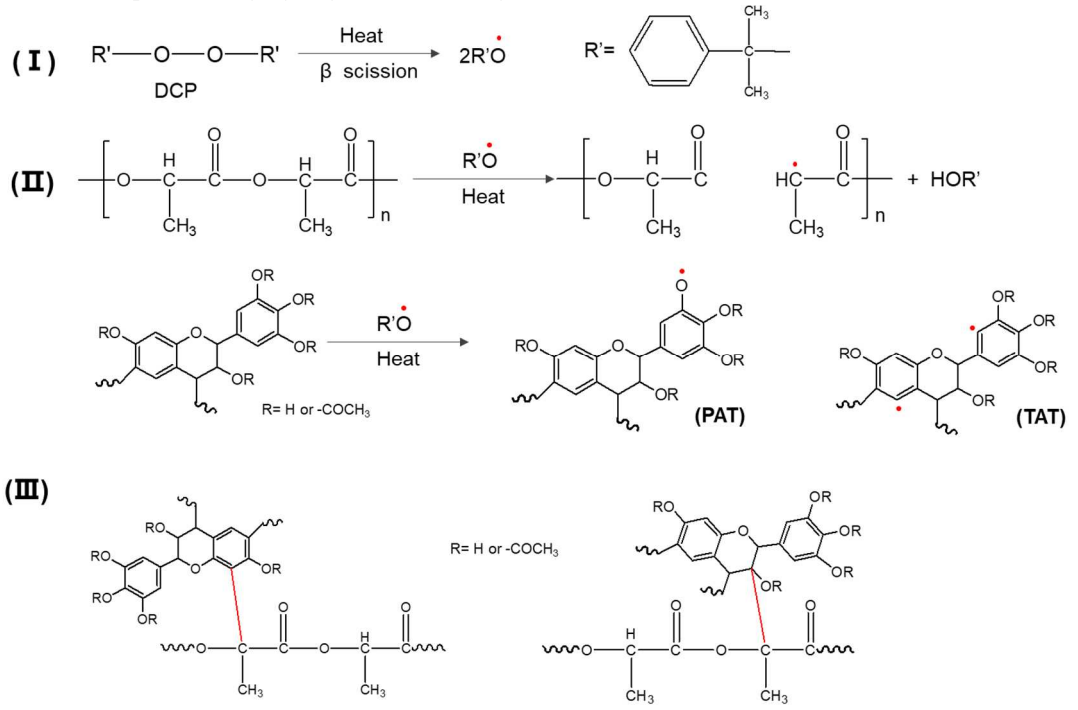

3.2. Mechanical property

The mechanical properties of PLA, PLA+DCP (PLD), PLA+PAT+DCP (PLPAT) and PLA+TAT+DCP (PLTAT) are presented in Figure 2. The control sample PLD display higher Young's modulus and tensile strength with a relatively low elongation compared with neat PLA because strong C-C chemical linkages initiated by DCP contributes to the formation of crosslinking structure between PLA chains (Yamoum et al., 2017). For filled polymer systems, where weak filler/matrix interfacial adhesion predominates, they show generally poor tensile strength due to poor stress transfer capacity between fillers and polymer matrix (Fu et al., 2008). In the presence of DCP,

the initiated PLA· radicals provided additional reacting sites for grafting with tannin acetate in different sites according to the acetylation degree (Scheme 1). This may result in the formation of more complex products such as cross-linked PLA polymer and PLA-tannin acetate copolymer. The intermolecular interactions between two components contributed to an enhanced stress transfer between two phases, thus, a relatively higher Young's modulus and tensile strength can be observed in PLPAT (3.8±0.1 GPa, 58±1.4 MPa), especially in PLTAT (4.2±0.1 GPa, 66±1 MPa) compared with PLA/tannin acetate blends without DCP (3.7±0.1 GPa, 52±2 MPa) in our previous study (Liao et al., 2020b). It is worth noting that the tensile properties of PLTAT is superior to PLD while that of PLPAT is comparable with PLD. This can be explained by the scavage capacity of phenolic OH groups limited the free radical polymerization since the generated phenoxy radicals (PhO·) is less active that prevents the initiation of new radicals in the polymer (Tolinski, 2015).

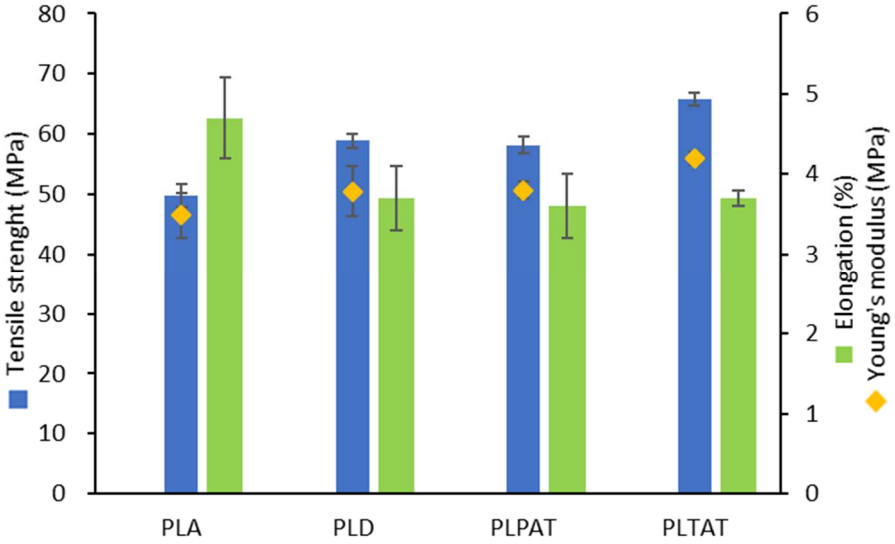

Figure 2. Tensile test results of PLA and reactive extruded samples using DCP

3.3. Molecular weight and rheological behaviour of PLA/AT blends using DCP

The reactive extruded samples were analysed by SEC and values of molecular weights ($\bar{M}_w$ and $\bar{M}_n$) and polydispersity index (PD, $\bar{M}_w/\bar{M}_n$) are reported in Table 2. Radical initiated polymerization of PLA and tannin acetate involves a series chemical reactions, including chain scission of PLA backbone, crosslinking of PLA chains and grafting copolymerization of PLA-tannin acetate (Monika et al., 2018; Yamoum et al., 2017). These reactions simutaneously occur in melt extrusion, promoting the generation of both the high- and low- molecular weight fration, therefore, a relatively

high PD was found in all reactive extruded samples compared with PLA. Compared with the extruded PLA, the depletion in the $\bar{M}_w$ and $\bar{M}_n$ values of reactive extruded samples was observed in Table 2, implying the thermal degradation was dominated during reactive extrusion; this phenomenon was commonly found in reactive extrusion using DCP (Monika et al., 2018). However, the chain scission of PLA caused by DCP radicals provide more reaction sites for the formation of covalent bonding in two phases (Yamoum et al., 2017), contributing to the improvement of interfacial adhesion of PLA/AT composites. A relatively low $\bar{M}_w$ and $\bar{M}_n$ values of PLPAT was observed in reactive extruded samples, which might blame to the generation of less active phenoxy radicals.

Table 2. SEC data of PLA and reactive extruded samples using DCP

	$\bar{M}_w$ (g/mol)	$\bar{M}_n$ (g/mol)	PD
PLA	1115000	1711000	0.65
PLD	304900	142800	2.14
PLPAT	213400	130200	1.64
PLTAT	386200	140000	2.76

The variation of the melt rheological properties is useful to investigate changes in molecular structure and interfacial adhesion property during the reactive extrusion (Yamoum et al., 2017). Figure 3 (a) shows the complex viscosity of reactive extruded samples as a function of angular frequency at 190 °C. The complex viscosity decreases with the increasing angular frequency, showing a shear thinning behaviour of PLA polymer in the resulting composites. DCP radicals promoted the chain scission of PLA polymer chain led to decrease of molecular weight in PLD, PLPAT and PLTAT (Table 2), thus a significant drop of complex viscosity of reactive extruded samples compared with PLA. As reported by Dorgan et al., PLA homopolymers with comparable molecular weights presents similar complex viscosity (Dorgan et al., 1999). One this basis, the introduction of filler in polymers was generally found a decrease of complex viscosity since the poor interfacial adhesion (Liao et al., 2020a, 2019a). In the case of PLPAT and PLTAT, their complex viscosity is much higher than that of PLD, referring the strong interfacial adhesion between PLA and tannin acetate in the presence of DCP. This phenomenon was commonly observed in polymer blends using DCP (Luo et al., 2016; Wei and

McDonald, 2015). Figure 3 (b) presents the storage modulus as a function of frequency of all tested samples, which corresponds to the elastic character of the blends or the energy stored during the deformation (Wei and McDonald, 2015). The domination of chain scission on PLD results in a drop of storage modulus due to the shorter polymer chains and less chains entanglement. In PLA/AT system, the presence of radicals induced covalent bonds between PLA and tannin acetate. The grafting between PLA and tannin acetate can increase the entanglement density, resulting in an increase of storage modulus (Dorgan et al., 1999). In the present study, the relatively lower storage modulus of PLPAT reveals most likely a less covalent linkage in PLA/PAT blending system. This can be explained by the presence of free phenolic –OH moieties of tannin acetate, which are competing to react with the DCP radicals. As a result, less grafting reactions can be undertaken between PLA and PAT.

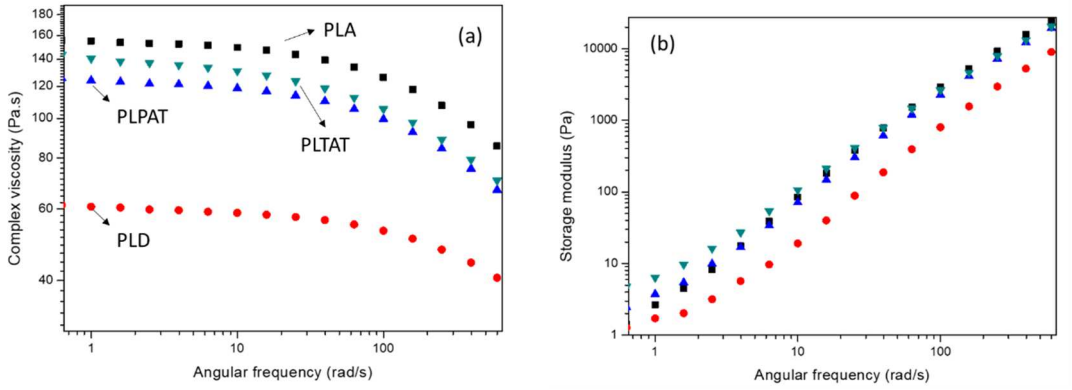

Figure 3. Rheological behavior of PLA and reactive extruded samples

3.4. Thermal behaviour

The temperature of glass transition (T_g), melt (T_m), cold crystalline (T_c), and degree of crystallinity (X_c) was investigated using DSC and the related data presented in Table 3. As reported in previous section, the molecular weight of extruded samples (PLD, PLPAT, PLTAT) in presence of DCP is lower than extruded PLA without DCP. Thus, PLD displayed relatively low grass transition, melting and cold crystal temperature. For PLA/AT with DCP, T_g shifted to a higher temperature compared with PLD, referring the formation of covalent bonding between PLA and tannin acetate since the mobility of polymer chain required more thermal energy (Wei and McDonald, 2015). PLPAT and PLTAT have a higher T_c because the introduction of tannin acetate in PLA and the generation of less regular polymer chains from radical

277 reaction results in the difficulty of chain reorganization and chain folding during
278 crystallization process (Dong et al., 2017). As chain scission of PLA backbone and
279 recombination of polymer chain occur simutaneously during the reactive extrusion
280 using DCP, the formation of inhomogeneous polymer chain segments inhibited the
281 crystallinity in PLD, PLA/AT blends. However, it should be noted that the X_c values
282 increased with the addition of tannin acetate, especially for PLTAT, which might due
283 to the improved interfacial adhesion of two components and dispersion of tannin
284 acetate in PLA matrix because of C-C grafting of PLA-AT (Dhar et al., 2016).

285 *Table 3. DSC data and weight loss of PLA and reactive extruded samples using DCP*

Samples	DSC				TAG-Weight loss (%)		
	T_g (°C)	T_c (°C)	T_{m1}; T_{m2} (°C)	X_c (%)	T_{90} (°C)	T_{max} (°C)	T_{10} (°C)
PLA	55.6	120.2	152.5; 162.8	7.4	322.8	357.5	367.2
PLD	55.1	116.3	149.6; 157.8	1.2	318.7	358.2	367.0
PLPAT	56.8	122.8	152.3; 161.6	2.1	316.8	352.2	370.3
PLTAT	57.0	121.5	150.8; 157.4	4.6	319.2	356.2	368.2

286 The thermal stability of PLA and reactive extruded samples was explored by
287 TGA under an air atmosphere and thermal degradation data was presented in Table 3.
288 The decomposition process of composites relies on the thermal stability of each
289 component, interfacial adhesion between the two components and molecular weight
290 of the polymer matrix (García et al., 2018; Yu et al., 2011). In our previous work, the
291 addition of PAT in PLA results in a decrease of thermal stability since the weak
292 interfacial adhesion between the filler and the polymer matrix (Liao et al., 2020b).
293 Thus, the degradation temperature of PLA/AT composites is comparable to PLA,
294 suggesting that interfacial adhesion of PLA and tannin acetate can be promoted by
295 free radical copolymerization.

296 **3.5. Contact angle analysis**

297 The wettability is an important property for PLA-based composites in the
298 application of food packaging for preventing the food items from humidity during
299 transport to the consumption stage (Monika et al., 2018). The wettability can be
300 characterized by depositing a water drop on the surface of material. Figure 4 is the
301 contact angle data of resulting samples at 1 s and 180 s. The contact angles of PLD
302 exhibited a higher contact angle compared with PLA either at 1 s or 180 s, indicating

reactive extruded PLD tend to be more hydrophobic than PLA. This might associate to covalent bonding of polymer chain initiated by free radicals. With the addition of tannin acetate, contact angles mainly rely on degree of roughness that will be affected by the dispersion of tannin acetate in PLA matrix. In our previous experiment, PLA blended with PAT generated a rough surface (Figure S2, supplementary material) because of the aggregation of tannin acetate. The dispersion of AT in PLA can be ameliorated via free radical copolymerization (Monika et al., 2018). The contact angle of PLPAT has a lower value compared with PLA + PAT (88° ± 1, Table S1, supplementary material), indicating good dispersion of tannin acetate in PLA. Therefore, it can be concluded from contact angle data, PLA/AT composites prepared by free radical copolymerization exhibited high degree of hydrophobicity, which are potentially applied in packaging applications.

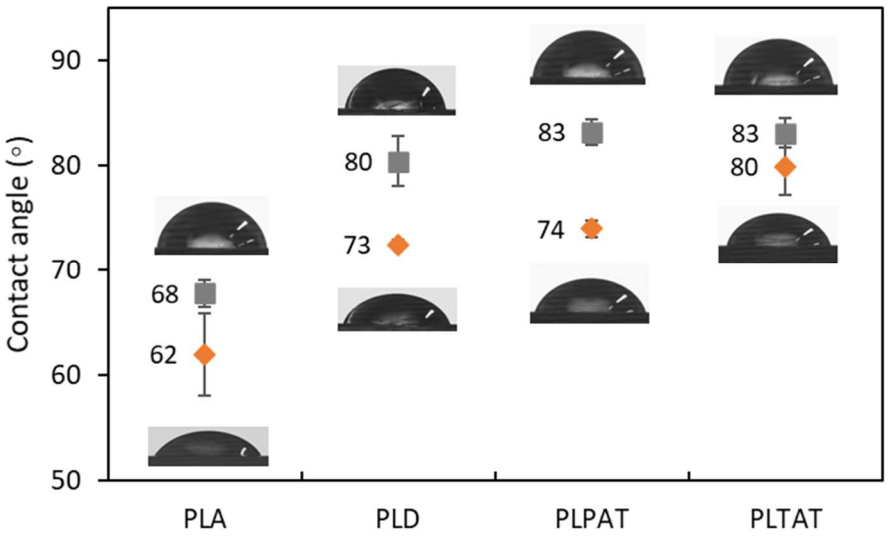

Figure 4. Contact angle at 1s (up) and 180 s (bottom) of PLA and reactive extruded samples at 25 ℃

4. Conclusions

In current work, PLA/AT composites have been prepared via in situ free radical copolymerization using DCP. The composites based on PLA and tannin acetate with high acetylation degree presented improved Young's modulus and tensile strengths as compared with PLA because the initiated DCP radicals contributed to the formation of covalent bonding between PLA and tannin acetate. The promoted intermolecular interaction of PLA/AT composites results from free radical

copolymerization, which can be investigated by the rheology test. The increased complex viscosity and modulus storage indicates the strong interfacial adhesion of PLA and tannin acetate. In addition, glass transition temperature, thermal stability and crystallinity degree of PLA/AT composites were all improved as a result of better interaction by free radical copolymerization. The enhanced hydrophobicity of PLA/AT composites may suggest a possible application towards packaging applications. It is expected that this free radical copolymerization can expand the application of tannin as a sustainable component for bio-composite preparation.

Acknowledgements

This work was supported by the National Natural Science Foundation of China (NSFC 31971595, 31760187) and the Program for Leading Talents of Science and Technology (grant No. 2017HA013) as well as the Yunnan Provincial Youth and Yunnan Provincial Reserve Talents for Middle & Young Academic and Technical Leaders (2019HB026). LERMAB is supported by the French National Research Agency through the Laboratory of Excellence ARBRE (ANR-12-LABXARBRE-01). China Scholarship Council is gratefully acknowledged. The authors also thank Richard Laine for precious technical support.

Notes

The authors declare no competing financial interest.

Reference:

Anwer, M.A.S., Naguib, H.E., Celzard, A., Fierro, V., 2015. Comparison of the thermal, dynamic mechanical and morphological properties of PLA-Lignin & PLA-Tannin particulate green composites. Composites Part B: Engineering 82, 92–99. https://doi.org/10.1016/j.compositesb.2015.08.028

Bridson, J.H., Grigsby, W.J., Main, L., 2018. One-pot solvent-free synthesis and characterisation of hydroxypropylated polyflavonoid compounds. Industrial Crops and Products 111, 529–535. https://doi.org/10.1016/j.indcrop.2017.11.028

Bridson, J.H., Grigsby, W.J., Main, L., 2013. Synthesis and characterization of flavonoid laurate esters by transesterification. J Appl Polym Sci 129, 181–186. https://doi.org/10.1002/app.38731

Dhar, P., Tarafder, D., Kumar, A., Katiyar, V., 2016. Thermally recyclable polylactic acid/cellulose nanocrystal films through reactive extrusion process. Polymer 87, 268–282. https://doi.org/10.1016/j.polymer.2016.02.004

Dong, J., Li, M., Zhou, L., Lee, S., Mei, C., Xu, X., Wu, Q., 2017. The influence of

363 grafted cellulose nanofibers and postextrusion annealing treatment on selected
364 properties of poly(lactic acid) filaments for 3D printing. Journal of Polymer
365 Science Part B: Polymer Physics 55, 847–855.
366 https://doi.org/10.1002/polb.24333
367 Dorgan, J.R., Williams, J.S., Lewis, D.N., 1999. Melt rheology of poly(lactic acid):
368 Entanglement and chain architecture effects. Journal of Rheology 43, 1141–
369 1155. https://doi.org/10.1122/1.551041
370 Fu, S.-Y., Feng, X.-Q., Lauke, B., Mai, Y.-W., 2008. Effects of particle size,
371 particle/matrix interface adhesion and particle loading on mechanical
372 properties of particulate–polymer composites. Composites Part B: Engineering
373 39, 933–961. https://doi.org/10.1016/j.compositesb.2008.01.002
374 García, D., Carrasco, J., Salazar, J., Pérez, M., Cancino, R., Riquelme, S., 2016. Bark
375 polyflavonoids from Pinus radiata as functional building-blocks for polylactic
376 acid (PLA)-based green composites. eXPRESS Polymer Letters 10, 835–848.
377 https://doi.org/10.3144/expresspolymlett.2016.78
378 García, D.E., Salazar, J.P., Riquelme, S., Delgado, N., Paczkowski, S., 2018.
379 Condensed Tannin-Based Polyurethane as Functional Modifier of PLA-
380 Composites. Polymer-Plastics Technology and Engineering 57, 709–726.
381 https://doi.org/10.1080/03602559.2017.1344855
382 Grigsby, W.J., Bridson, J.H., Lomas, C., Elliot, J.-A., 2013. Esterification of
383 Condensed Tannins and Their Impact on the Properties of Poly(Lactic Acid).
384 polymers 5, 334–360. https://doi.org/10.3390/polym5020344
385 Grigsby, W.J., Bridson, J.H., Lomas, C., Frey, H., 2014. Evaluating Modified Tannin
386 Esters as Functional Additives in Polypropylene and Biodegradable Aliphatic
387 Polyester: Modified Tannin Esters as Plastic Additives. Macromol. Mater. Eng.
388 299, 1251–1258. https://doi.org/10.1002/mame.201400051
389 Grigsby, W.J., Kadla, J.F., 2014. Evaluating Poly(lactic acid) Fiber Reinforcement
390 with Modified Tannins: Evaluating Poly(lactic acid) Fiber Reinforcement ….
391 Macromol. Mater. Eng. 299, 368–378.
392 https://doi.org/10.1002/mame.201300174
393 Jiang, S., 2017. Blending PLLA/tannin-grafted PCL fiber membrane for skin tissue
394 engineering. J Mater Sci 8.
395 Karkhanis, S.S., Stark, N.M., Sabo, R.C., Matuana, L.M., 2018. Water vapor and
396 oxygen barrier properties of extrusion-blown poly(lactic acid)/cellulose
397 nanocrystals nanocomposite films. Composites Part A: Applied Science and
398 Manufacturing 114, 204–211.
399 https://doi.org/10.1016/j.compositesa.2018.08.025
400 Kumar, A., Tumu, V.R., Ray Chowdhury, S., S.v.s., R.R., 2019. A green physical
401 approach to compatibilize a bio-based poly (lactic acid)/lignin blend for better
402 mechanical, thermal and degradation properties. International Journal of
403 Biological Macromolecules 121, 588–600.
404 https://doi.org/10.1016/j.ijbiomac.2018.10.057
405 Liao, J., Brosse, N., Hoppe, S., Du, G., Zhou, X., Pizzi, A., 2020a. One-step
406 compatibilization of poly(lactic acid) and tannin via reactive extrusion.
407 Materials & Design 191, 108603.
408 https://doi.org/10.1016/j.matdes.2020.108603
409 Liao, J., Brosse, N., Pizzi, A., Hoppe, S., 2019a. Dynamically Cross-Linked Tannin as
410 a Reinforcement of Polypropylene and UV Protection Properties. Polymers 11,
411 102. https://doi.org/10.3390/polym11010102
412 Liao, J., Brosse, N., Pizzi, A., Hoppe, S., Xi, X., Zhou, X., 2019b. Polypropylene

Blend with Polyphenols through Dynamic Vulcanization: Mechanical, Rheological, Crystalline, Thermal, and UV Protective Property. Polymers 11, 1108. https://doi.org/10.3390/polym11071108

Liao, J., Brosse, N., Pizzi, A., Hoppe, S., Zhou, X., Du, G., 2020b. Characterization and 3D printability of poly (lactic acid)/acetylated tannin composites. Industrial Crops and Products 149, 112320. https://doi.org/10.1016/j.indcrop.2020.112320

Luo, C., Grigsby, W., Edmonds, N., Easteal, A., Al-Hakkak, J., 2010. Synthesis, characterization, and thermal behaviors of tannin stearates prepared from quebracho and pine bark extracts. Journal of Applied Polymer Science 117, 352–360. https://doi.org/10.1002/app.31545

Luo, C., Grigsby, W.J., Edmonds, N.R., Al-Hakkak, J., 2014. Rubber-Like Materials Prepared from Copolymerization of Tannin Fatty Acid Conjugates and Vegetable Oils. Macromolecular Materials and Engineering 299, 65–74. https://doi.org/10.1002/mame.201300039

Luo, C., Grigsby, W.J., Edmonds, N.R., Al-Hakkak, J., 2013. Vegetable oil thermosets reinforced by tannin–lipid formulations. Acta Biomaterialia 9, 5226–5233. https://doi.org/10.1016/j.actbio.2012.08.048

Luo, S., Cao, J., McDonald, A.G., 2018. Cross-linking of technical lignin via esterification and thermally initiated free radical reaction. Industrial Crops and Products 121, 169–179. https://doi.org/10.1016/j.indcrop.2018.05.007

Luo, S., Cao, J., McDonald, A.G., 2016. Interfacial Improvements in a Green Biopolymer Alloy of Poly(3-hydroxybutyrate-co-3-hydroxyvalerate) and Lignin via in Situ Reactive Extrusion. ACS Sustainable Chem. Eng. 4, 3465–3476. https://doi.org/10.1021/acssuschemeng.6b00495

Monika, Pal, A.K., Bhasney, S.M., Bhagabati, P., Katiyar, V., 2018. Effect of Dicumyl Peroxide on a Poly(lactic acid) (PLA)/Poly(butylene succinate) (PBS)/Functionalized Chitosan-Based Nanobiocomposite for Packaging: A Reactive Extrusion Study. ACS Omega 3, 13298–13312. https://doi.org/10.1021/acsomega.8b00907

Nicollin, A., Zhou, X., Pizzi, A., Grigsby, W., Rode, K., Delmotte, L., 2013. MALDI-TOF and 13C NMR analysis of a renewable resource additive—Thermoplastic acetylated tannins. Industrial Crops and Products 49, 851–857. https://doi.org/10.1016/j.indcrop.2013.06.013

Pizzi, A., 1980. Tannin-Based Adhesives. Journal of macromolecular science 18, 247–315.

Quideau, S., Deffieux, D., Douat-Casassus, C., Pouysegu, L., 2011. Plant polyphenols: chemical properties, biological activities, and synthesis. Angewandte Chemie International Edition 50, 586–621.

Ren, J., 2011. Biodegradable Poly(Lactic Acid): Synthesis, Modification, Processing and Applications. Springer Berlin Heidelberg, Berlin, Heidelberg. https://doi.org/10.1007/978-3-642-17596-1

Song, P., Jiang, S., Ren, Y., Zhang, X., Qiao, T., Song, X., Liu, Q., Chen, X., 2016. Synthesis and characterization of tannin grafted polycaprolactone. Journal of Colloid and Interface Science 479, 160–164. https://doi.org/10.1016/j.jcis.2016.06.056

Song, Y., Zong, X., Wang, N., Yan, N., Shan, X., Li, J., 2018. Preparation of γ-Divinyl-3-Aminopropyltriethoxysilane Modified Lignin and Its Application in Flame Retardant Poly(lactic acid). Materials 11, 1505. https://doi.org/10.3390/ma11091505

Thébault, M., Pizzi, A., Essawy, H.A., Barhoum, A., Van Assche, G., 2015. Isocyanate free condensed tannin-based polyurethanes. European Polymer Journal 67, 513–526. https://doi.org/10.1016/j.eurpolymj.2014.10.022

Tolinski, M., 2015. Additives for polyolefins: getting the most out of polypropylene, polyethylene and TPO, Second edition. ed, PDL handbook series. Elsevier, William Andrew is an imprint of Elsevier, Kidlington, Oxford, UK.

Wei, L., McDonald, A.G., 2015. Peroxide induced cross-linking by reactive melt processing of two biopolyesters: Poly(3-hydroxybutyrate) and poly(l-lactic acid) to improve their melting processability. Journal of Applied Polymer Science 132. https://doi.org/10.1002/app.41724

Wei, L., McDonald, A.G., Stark, N.M., 2015. Grafting of Bacterial Polyhydroxybutyrate (PHB) onto Cellulose via In Situ Reactive Extrusion with Dicumyl Peroxide. Biomacromolecules 10.

Yamoum, C., Maia, J., Magaraphan, R., 2017. Rheological and thermal behavior of PLA modified by chemical crosslinking in the presence of ethoxylated bisphenol A dimethacrylates: Rheological and Thermal Behaviors of PLA with Bis-EMA Crosslinking. Polym. Adv. Technol. 28, 102–112. https://doi.org/10.1002/pat.3864

Yang, W., Weng, Y., Puglia, D., Qi, G., Dong, W., Kenny, J.M., Ma, P., 2020. Poly(lactic acid)/lignin films with enhanced toughness and anti-oxidation performance for active food packaging. International Journal of Biological Macromolecules 144, 102–110. https://doi.org/10.1016/j.ijbiomac.2019.12.085

Yu, H.-Y., Zhang, H., Song, M.-L., Zhou, Y., Yao, J., Ni, Q.-Q., 2017. From Cellulose Nanospheres, Nanorods to Nanofibers: Various Aspect Ratio Induced Nucleation/Reinforcing Effects on Polylactic Acid for Robust-Barrier Food Packaging. ACS Appl. Mater. Interfaces 9, 43920–43938. https://doi.org/10.1021/acsami.7b09102

Yu, L., Petinakis, E., Dean, K., Liu, H., Yuan, Q., 2011. Enhancing compatibilizer function by controlled distribution in hydrophobic polylactic acid/hydrophilic starch blends. Journal of Applied Polymer Science 119, 2189–2195. https://doi.org/10.1002/app.32949

Zhou, L., He, H., Li, M., Huang, S., Mei, C., Wu, Q., 2018. Enhancing mechanical properties of poly(lactic acid) through its in-situ crosslinking with maleic anhydride-modified cellulose nanocrystals from cottonseed hulls. Industrial Crops and Products 112, 449–459. https://doi.org/10.1016/j.indcrop.2017.12.044

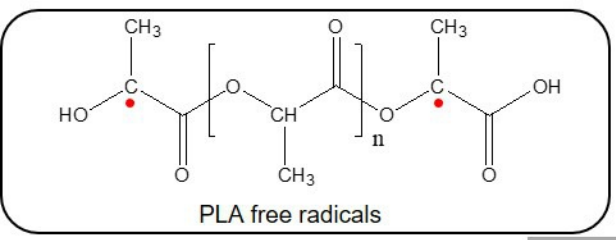
PLA free radicals

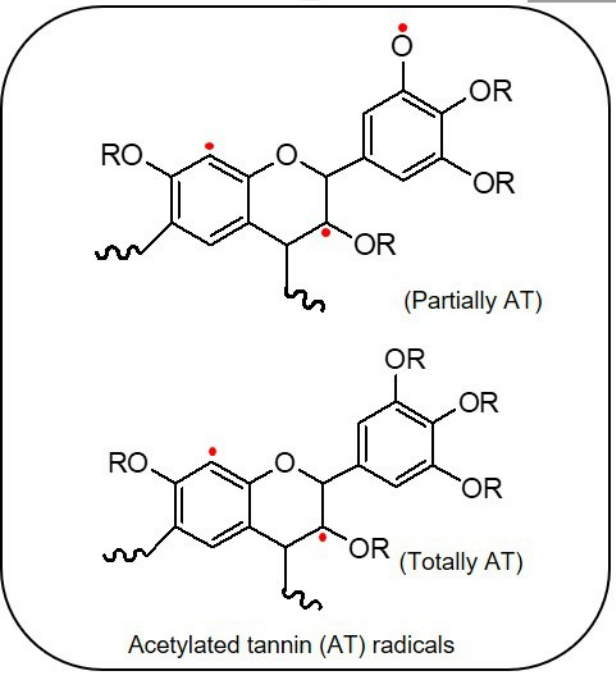
(Partially AT)
(Totally AT)
Acetylated tannin (AT) radicals

Extrusion

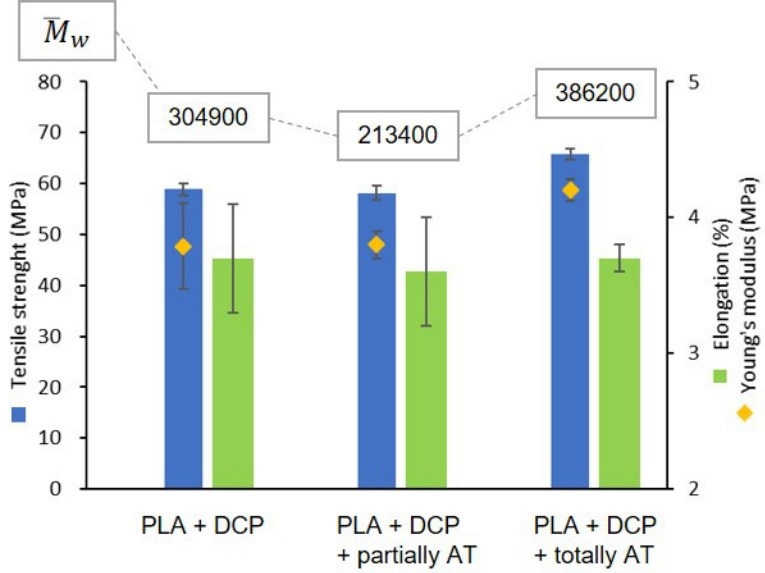
$\bar{M}_w$
304900
213400
386200
Tensile strenght (MPa)
Elongation (%)
Young's modulus (MPa)
PLA + DCP
PLA + DCP + partially AT
PLA + DCP + totally AT

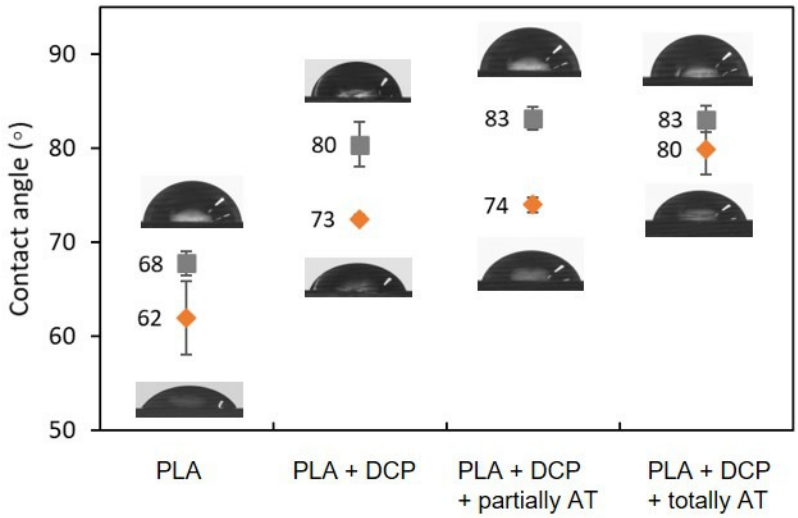
Contact angle (°)
68
62
80
73
83
74
83
80
PLA
PLA + DCP
PLA + DCP + partially AT
PLA + DCP + totally AT